THE ASTROPHYSICAL JOURNAL, 317:271–281, 1987 June 1

ABERRATION AND ADVECTION EFFECTS IN A PLANE-PARALLEL MEDIUM IN MOTION

A. PERAIAH
Indian Institute of Astrophysics, Bangalore, India
Received 1986 May 12; accepted 1986 October 28

ABSTRACT

We have considered the effects of the aberration and advection terms in the radiative transfer equation. We employed a plane-parallel medium which is moving with velocities 1000, 2000, 3000, 4000, or 5000 km s^{-1} ($\beta \approx 0.0033$–0.017, where $\beta = V/C$; V is the velocity of the gas and C is the velocity of light). The calculations have been done in the fluid frame, with a monochromatic radiation field. We assumed no internal emissions, and isotropic scattering is the only physical process that is assumed to operate in the fluid.

We calculated the effects of the aberration and advection terms on mean intensities and on outward fluxes for different velocities (both positive and negative) and optical depths. It is found that for an optical depth of $\tau = 1$, the maximum deviation in $\bar{J}$ $\{= [J(V = 0) - J(V > 0)]/J(V = 0)\}$, where $\bar{J}$ is the mean intensity, $\bar{F}$ $\{= [F(V = 0) - F(V > 0)]/F(V = 0)\}$, where F is the outward flux, at $\beta = +0.017$, will be $\sim 6\%$. But when optical depths increase, the deviations in mean intensity and outward fluxes are considerably enhanced. At $\tau = 5$, $\bar{J} \approx 11\%$–12%; at $\tau = 10$, $\bar{J} \approx 20\%$; and at $\tau = 50$, $\bar{J} \approx 80\%$–90%. When negative velocities are employed, we obtain $\bar{J} \approx -5\%$ for $\tau = 1$ with $\beta \approx 0.0167$, and $\bar{J} = -160\%$ for $\tau = 50$ with $\beta = -0.0167$. Similar values for $\bar{F}$ corresponding to the same parameters of τ and β are obtained. The amplification factors defined as $\bar{J}_{max}/100\beta$ and $\bar{F}_{max}/100\beta$ are found to vary almost linearly with the total thickness of the slab. We therefore feel that the aberration and advection terms should be properly considered in evaluating the radiation field in a moving medium.

Subject heading: radiative transfer

I. INTRODUCTION

It is well known that the matter in the outer layers of some supergiant stars, novae, supernovae, quasi-stellar objects, etc., are moving with large velocities. The velocities of expansion or contraction are so large that the velocity of light cannot be infinite in comparison. In such situations, we have to consider the effects of aberration and advection generated by the high velocities on the radiation field. These effects have been included in radiative transfer by Mihalas, Kunasz, and Hummer (1976), and it is found that the effects of aberration and advection are small when velocities of the order $V/C \approx 0.01$ are considered, and that the Doppler shifts in the frequency derivative term are the only important parameters in changing the radiation field. Mihalas and Klein (1982) have shown that the terms $O(V/C)$ should be retained in the time-dependent radiative transfer equation.

In this paper, we have made an attempt to solve the time-independent radiative transfer equation in the fluid frame with the aberration and advection terms included, retaining the terms to $O(V/C)$. We assumed a plane-parallel medium with coherent isotropic scattering and no creation or destruction of photons within the medium. It appears from these calculations that the terms of the $O(V/C)$ introduce substantial changes in the mean intensities and the outward fluxes even when time dependency is ignored. We have employed the method described in Peraiah and Varghese (1985, hereafter Paper I).

In the next section we shall give a brief description of the method, and results are presented in § III.

II. DESCRIPTION OF THE METHOD OF OBTAINING SOLUTION

The monochromatic, plane-parallel, steady state radiative transfer equation in a fluid frame (Castor 1972; Mihalas 1978; Munier and Weaver 1986) with aberration and advection terms is given by

$$(\mu + \beta)\frac{\partial I(z,\mu)}{\partial z} + \frac{\mu(\mu^2 - 1)}{c}\frac{\partial v}{\partial z}\frac{\partial I(z,\mu)}{\partial \mu} + \frac{3\mu^2}{c}\frac{\partial v}{\partial z}I(z,\mu) = K[S - I(z,\mu)] , \tag{1}$$

where $\mu = (\mu' - \beta)/(1 - \mu'\beta)$, and μ' $(0 \le \mu' \le 1)$ is the cosine of the angle made by the ray with the Z-axis; $\beta = V/C$; V is the velocity of the fluid and C is the velocity of light; $I(z, \mu)$ is the specific intensity of the ray; K is the absorption coefficient; and S is the source function. In this case it is given by

$$S = \tfrac{1}{2}\int_{-1}^{+1} P(z, \mu_1', \mu_2')I(z, \mu_2')\, d\mu_2' . \tag{2}$$

We integrate equation (1) as described in Paper I. We expand the specific intensity as

$$I = I_0 + \xi I_z + \eta I_\mu + \xi\eta I_{z\mu} , \tag{3}$$

where I_0, I_z, I_μ, and $I_{z\mu}$ are the interpolation coefficients, and

$$\xi = \frac{z - \bar{z}}{\Delta z/2} , \qquad \eta = \frac{\mu - \bar{\mu}}{\Delta\mu/2} , \tag{4}$$

where

$$\bar{z} = \tfrac{1}{2}(z_i + z_{i-1}), \qquad \Delta z = (z_i - z_{i-1}), \tag{5}$$

and

$$\bar{\mu} = \tfrac{1}{2}(\mu_j + \mu_{j-1}), \qquad \Delta\mu = (\mu_j - \mu_{j-1}); \tag{6}$$

z_i, z_{i-1} and μ_j, μ_{j-1} are the discrete points along the z–μ grid.

We substitute equation (3) into equation (1) and integrate the resulting equation over the z–μ grid. We thus obtain

$$\frac{2}{\Delta z}(\bar{\mu} + \beta)I_z + (g + \Delta\mu\bar{\mu})\frac{d\beta}{dz}I_\mu + \frac{1}{3}\Delta\mu I_{z\mu} + \left(k + 3\overline{\mu^2}\frac{d\beta}{dz}\right)I_0 = KS_0;$$

similarly, for the equation for $-1 < \mu < 0$, we have

$$\frac{2}{\Delta z}(\beta - \bar{\mu})I_z + (g + \Delta\mu\bar{\mu})\frac{d\beta}{dz} - \frac{1}{3}\Delta\mu I_{z\mu} + \left(k + 3\overline{\mu^2}\frac{d\beta}{dz}\right) = KS_0, \tag{8}$$

where we have assumed that $d\beta/dz$ is constant over the interval (z_i, z_{i-1}), and

$$\overline{\mu^2} = (\bar{\mu})^2 + \tfrac{1}{12}(\Delta\mu)^2, \tag{9}$$

$$g = \frac{2\bar{\mu}}{\Delta\mu}(\langle\mu^2\rangle - 1), \tag{10}$$

$$\langle\mu^2\rangle = \tfrac{1}{2}(\mu_j^2 + \mu_{j-1}^2). \tag{11}$$

The interpolation coefficients $I_0, I_z, I_\mu, I_{z\mu}$ are replaced by their corresponding nodal values (see Paper I). Thus equations (7) and (8) become

$$A_a I_{j-1}^{i-1,+} + A_b I_j^{i-1,+} + A_c I_{j-1}^{i,+} + A_d I_j^{i,+} = \tau(S_{j-1}^{i-1,+} + S_j^{i-1,+} + S_{j-1}^{i,+} + S_j^{i,+}), \tag{12}$$

$$A'_a I_{j-1}^{i-1,-} + A'_b I_j^{i-1,-} + A'_c I_{j-1}^{i,-} + A'_d I_j^{i,-} = \tau(S_{j-1}^{i-1,-} + S_j^{i-1,-} + S_{j-1}^{i,-} + S_j^{i,-}), \tag{13}$$

where

$$I_{j-1}^{i-1,+} = I(z_{i-1}, \ +\mu_{j-1}), \quad \text{etc.}, \tag{14}$$

$A_a, A_b, A_c, A_d, A'_a, A'_b, A'_c$, and A'_d are given in Appendix A, and

$$S_{j-1}^{i-1,+} = \Sigma\tfrac{1}{2}(P^{++}CI^{i-1,+} + P^{+-}CI^{i-1,-})_{j-1}; \tag{15}$$

τ is the optical depth, given by

$$\Delta\tau = K\Delta z. \tag{16}$$

We can write similarly $S_j^{i,+}$, etc.

Equations (12) and (13) can be rewritten for J-angles. Thus we have (see Paper I)

$$(\boldsymbol{A}^{cd} - \tau\boldsymbol{Q}\gamma^{++})\boldsymbol{I}_i^+ + (\boldsymbol{A}^{ab} - \tau\boldsymbol{Q}\gamma^{++})\boldsymbol{I}_{i-1}^+ = \tau\boldsymbol{Q}\gamma^{+-}\boldsymbol{I}_i^- + \tau\boldsymbol{Q}\gamma^{+-}\boldsymbol{I}_{i-1}^-, \tag{17}$$

and

$$(\boldsymbol{A}'^{cd} - \tau\boldsymbol{Q}\gamma^{--})\boldsymbol{I}_i^- + (\boldsymbol{A}'^{ab} - \tau\boldsymbol{Q}\gamma^{--})\boldsymbol{I}_{i-1}^- = \tau\boldsymbol{Q}\gamma^{-+}\boldsymbol{I}_i^+ + \tau\boldsymbol{Q}\gamma^{-+}\boldsymbol{I}_{i-1}^+, \tag{18}$$

where

$$\{Q_{jj}, Q_{j,j+1}\} = 1, \tag{19}$$

and

$$\boldsymbol{A}^{ab} = \begin{bmatrix} A_a^{j-1} & A_b^j & & & \\ & A_a^j & A_b^{j+1} & & \\ & & \ddots & \ddots & \\ & & & A_a^{J-1} & A_b^J \\ & & & & A_a^J \end{bmatrix}. \tag{20}$$

Other matrices $\boldsymbol{A}^{cd}$, $\boldsymbol{A}'^{ab}$, $\boldsymbol{A}'^{cd}$ are defined similarly:

$$\gamma^{++} = \tfrac{1}{2}P^{++}C, \quad \text{etc.}; \tag{21}$$

$$P^{++} = P(+\mu, \ +\mu), \quad \text{etc.} \tag{22}$$

From equations (17) and (18) we can obtain the transmission and reflection operators (see the procedure described in Paper I or in Peraiah 1984). These operators are described in Appendix B. We employed the formula in Appendix B to obtain the radiation field in a plane-parallel medium which is in motion. The results are presented in the next section.

III. RESULTS AND DISCUSSION

We considered a medium in plane-parallel stratification and derived results which show that the effects due to velocities on the order of V/C are important. For this purpose, we consider a plane-parallel slab bounded by $\tau = \tau_{max}$ and $\tau = 0$, where τ is the optical depth. The medium is nonemitting, and isotropic scattering is the only physical process that is assumed to be operating in the medium. Therefore we apply the following boundary conditions:

$$I^{-}(\tau = \tau_{max}, \mu_j) = 1 , \tag{23}$$

$$I^{+}(\tau = 0, \mu_j) = 0 . \tag{24}$$

The physical meaning of equations (23) and (24) is that we irradiate the slab at $\tau = \tau_{max}$ with a unit intensity, and no radiation is incident at $\tau = 0$. The velocity gradient $dV/d\tau$ is constant. For each model, with $dV/d\tau < 0$, the boundary conditions on velocity are given by

$$V(\tau = \tau_{max}) = 0 , \tag{25}$$

$$V(\tau = 0) = V , \tag{26}$$

where

$V = 0$ km s^{-1} ($\beta = 0$), 1000 km s^{-1} ($\beta = 0.0033$), 2000 km s^{-1} ($\beta = 0.0067$), 3000 km s^{-1} ($\beta = 0.01$), 4000 km s^{-1} ($\beta = 0.013$), 5000 km s^{-1} ($\beta = 0.0167$).

The optical depths τ_{max} are taken to be

$$\tau_{max} = 1, 15, 10, 30, \text{and } 50 . \tag{27}$$

Mean intensities and the outward fluxes are computed as follows:

$$J = \tfrac{1}{2} \int_{-1}^{+1} I(\mu)\, d\mu , \tag{28}$$

and

$$F = \int_{0}^{1} I(\mu)\mu\, d\mu . \tag{29}$$

The changes in J and F due to velocities compared to those calculated without velocities are estimated. Thus

$$\bar{J} = \frac{\Delta J}{J(V = 0)} \times 100 , \tag{30}$$

$$\bar{F} = \frac{\Delta F}{F(V = 0)} \times 100 , \tag{31}$$

where

$$\Delta J = J(V = 0) - J(V > 0) , \tag{32}$$

$$\Delta F = F(V = 0) - F(V > 0) . \tag{33}$$

With the boundary conditions given in equations (23) and (24), we can solve equation (1). We employed four Radau's points on $\mu \in (0, 1)$. The solution is tested by observing the principle of conservation of flux. In plane-parallel stratification this is done easily, by obtaining positive transmission and reflection matrices (see Appendix B). The medium is divided into several layers, for each of which r and t matrices are estimated. By using these quantities we calculate the internal radiation field and flux conservation (Peraiah 1984). If we find that the flux conservation is not satisfied, then we subdivide each layer and recalculate the flux conservation. This process is continued until the condition of flux conservation is satisfied. When velocities are introduced, we may have to reduce the size of the layer so that we still obtain correct solutions that satisfy the condition of flux conservation. With small velocities ($V \approx$ 1000–3000 km s^{-1}), there is little difficulty, even for maximum optical depths of 50, in obtaining correct solutions. When velocities are increased to 5000 km s^{-1}, the accuracy starts declining at larger optical depths, although it still remains within the limits of acceptable error limits. In double precision we may obtain the flux conservation to 1 in 10^{-14} or 10^{-15} (the machine accuracy), and at high velocities and large optical depths the flux can be conserved to 1 in 10^{-7} to 10^{-8}. However, this can be improved by taking thinner and thinner (optically) layers at the expense of computer time.

It will be interesting to know the individual effects of aberration and advection separately. However, it is difficult to separate the terms corresponding to these two phenomena in equation (1). In equation (1), the first term on the left-hand side represents aberration, while the second and third terms represent both abberation and advection. It is difficult to define explicitly the terms representing aberration and advection. However, we shall approximately set the following conditions for aberration and advection, although they are very artificial:

$$\frac{d\beta}{dz} = 0, \beta \gtrless 0 , \quad \text{for aberration and no advection ;} \tag{34}$$

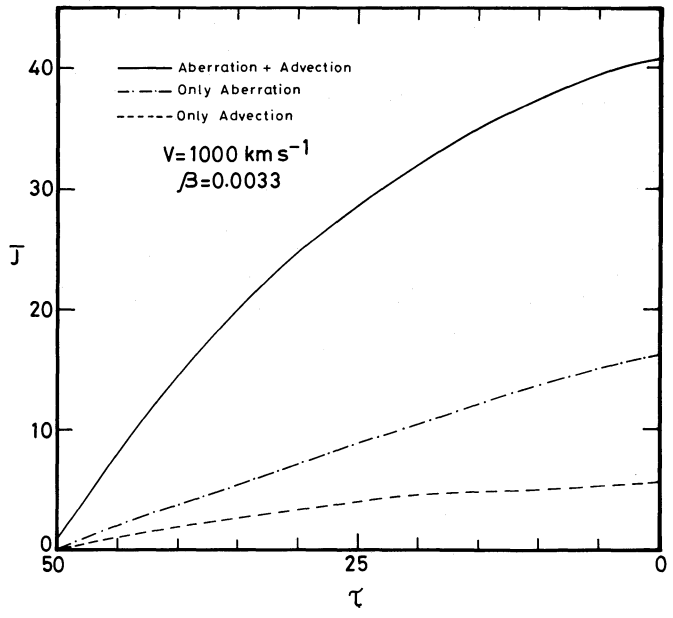

FIG. 1

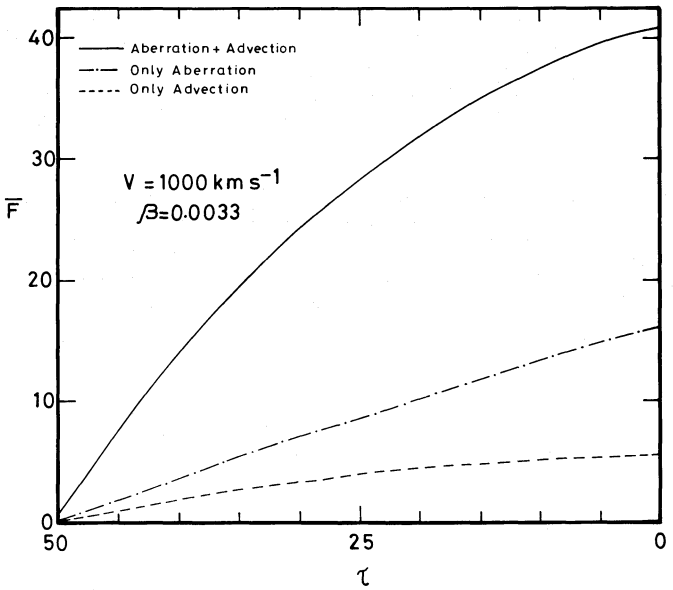

FIG. 2

FIG. 1.—Values of $\bar{J}$ plotted separately (see eqs. [34] and [35]) for advection and aberration effects for $V = 1000$ km s^{-1} for $\tau_{max} = 50$

FIG. 2.—Values of $\bar{F}$ plotted separately for $V = 1000$ km s^{-1} and $\tau_{max} = 50$

and

$$\frac{d\beta}{dz} \gtrless 0, \beta = 0 , \qquad \text{for advection and no aberration .} \tag{35}$$

We plot the mean intensities $\bar{J}$ and outward fluxes $\bar{F}$ produced by aberration and advection individually and the net effect in Figures 1 and 2 for $\tau = 50$ and $v = 5000$ km s^{-1} ($\beta \approx 0.0033$) and in Figures 3 and 4 for $\tau = 50$ and $v = 5000$ km s^{-1} ($\beta \approx 0.0167$). Advection changes $\bar{J}$ and $\bar{F}$ by $\sim 5\%$ each, while the changes due to aberration are $\sim 16\%$ each. However, the combined effect, obtained by including all three terms on the left-hand side of equation (1) due to aberration and advection, is more than 40%, much larger than the sum of the two effects calculated according to equations (34) and (35). This is not surprising, because when we include the three terms on the left-hand side of equation (1) in the calculations, we are not only taking the individual terms corresponding to aberration and advection but also the terms containing the combination of these two phenomena, and this results in values different from those obtained by the approximations described in equations (34) and (35).

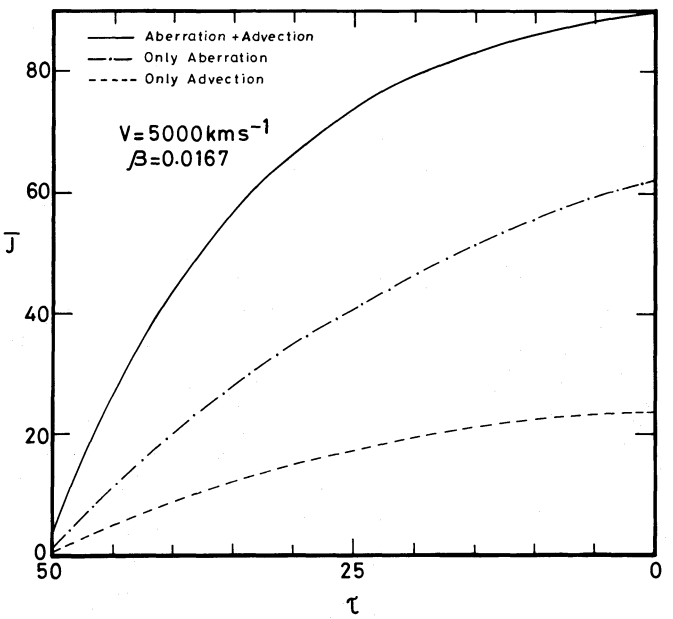

FIG. 3.—Same as Fig. 1, with $V = 5000$ km s^{-1}

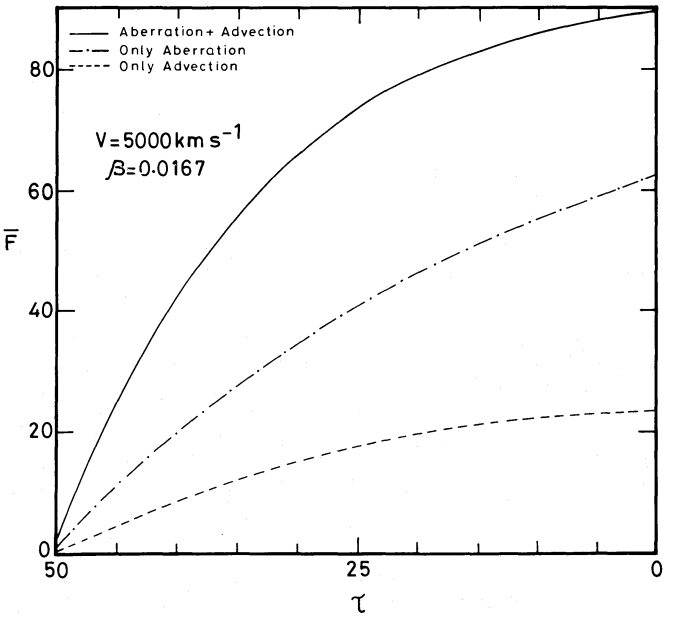

FIG. 4.—Same as Fig. 2, with $V = 5000$ km s^{-1}

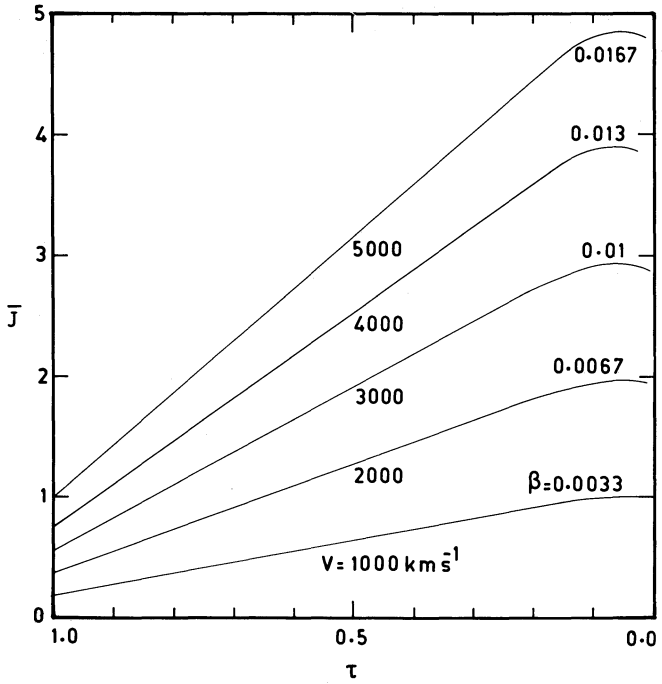

FIG. 5.—$\bar{J}$ plotted for $V = 1000, 2000, 3000, 4000$, and 5000 km s^{-1} for $\tau_{max} = 1$

In Figures 5 and 6 we plot the quantities $\bar{J}$ and $\bar{F}$ for different values of V (see eq. [27]), $\tau_{max} = 1$. For $V = 1000$ km s^{-1} ($\beta \approx 3 \times 10^{-3}$), the changes are less than 1%. But as V is increased to 5000 km s^{-1} ($\beta = 0.0167$), the changes $\bar{J}$ and $\bar{F}$ are considerable and reach as much as 5%–6%. When τ_{max} is increased to 5, $\bar{J}$ and $\bar{F}$ at 1000 km s^{-1} increase to $\sim$2%, but at $V = 5000$ km s^{-1}, they become 11%–12% (see Figs. 7 and 8). This is a change that cannot be neglected in the estimation of radiation field. For $\tau_{max} = 10$, the changes in $\bar{J}$ and $\bar{F}$ become as much as 20%, as shown in Figures 9 and 10. In Figures 11–14 the results of $\bar{J}$ and $\bar{F}$ for $\tau_{max} = 30$ and 50 are given. We can see that there are substantial changes in $\bar{J}$ and $\bar{F}$ even at $V = 1000$ km s^{-1} ($\beta \approx 0.0033$); at $V = 5000$ km s^{-1}, $\bar{J}$ and $\bar{F}$ become nearly 90%.

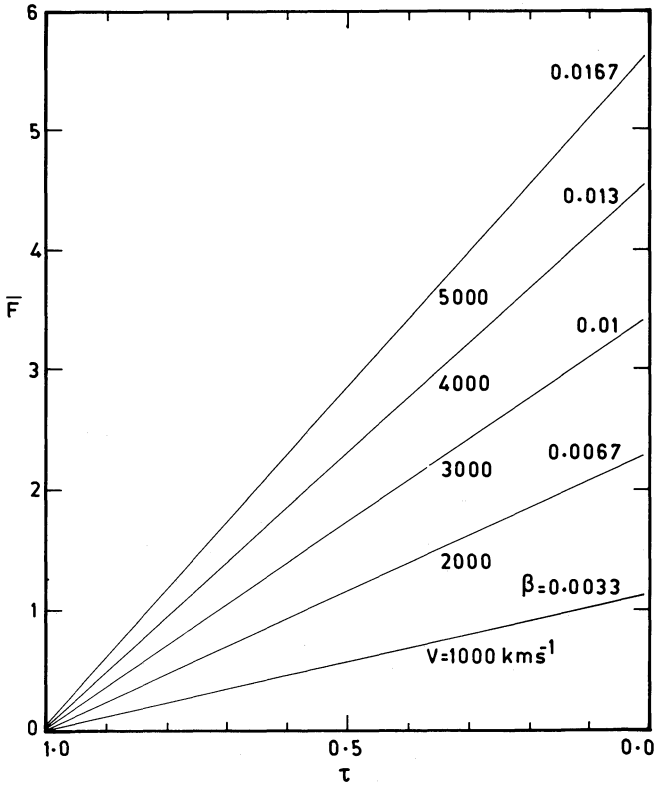

FIG. 6.—$\bar{F}$ plotted for $\tau_{max} = 1$ for positive velocities

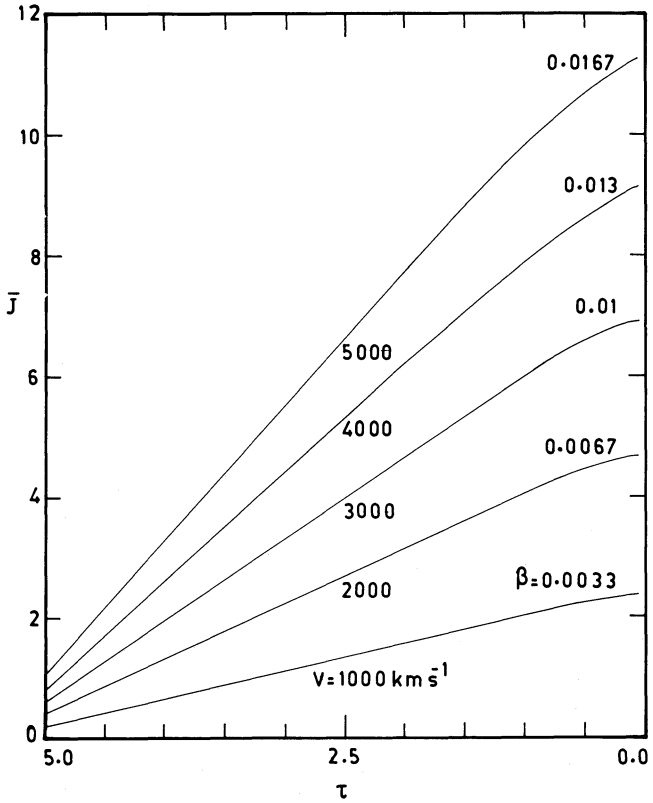

FIG. 7.—$\bar{J}$ plotted for $\tau_{max} = 5$ for positive velocities

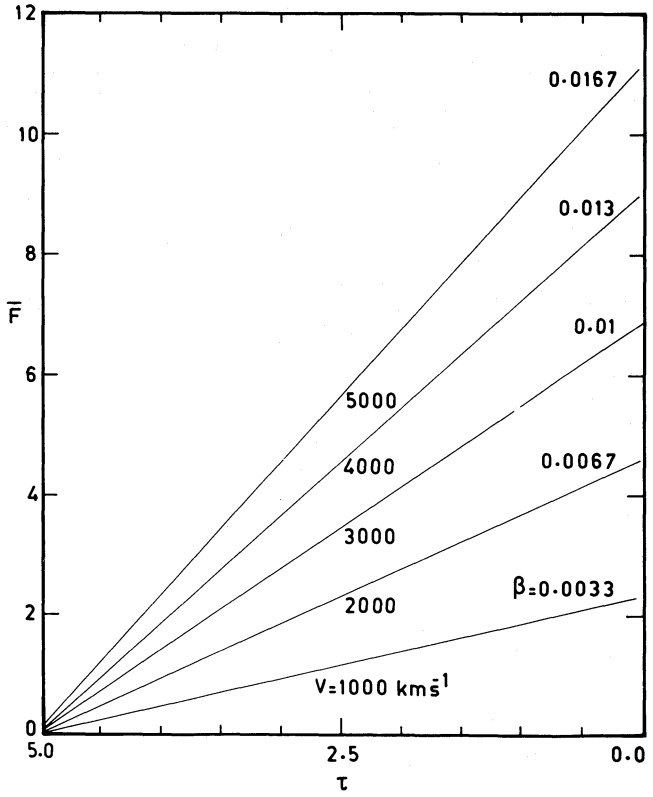

FIG. 8.—$\bar{F}$ plotted for $\tau_{max} = 5$ for positive velocities

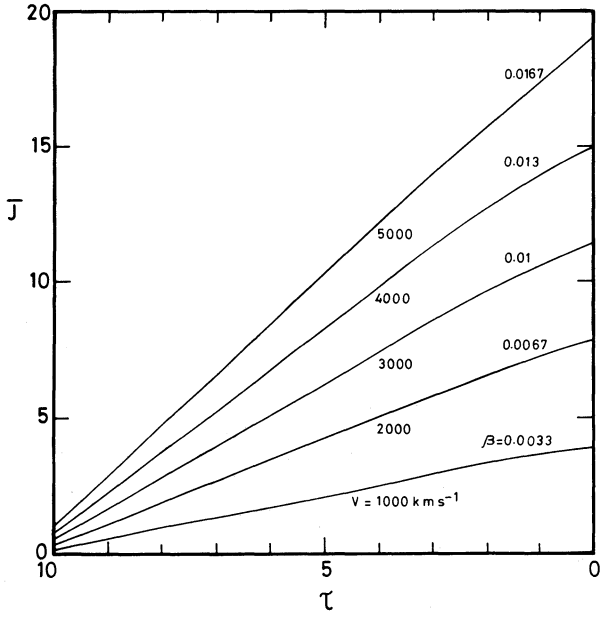

FIG. 9.—$\bar{J}$ plotted for $\tau_{max} = 10$ for positive velocities

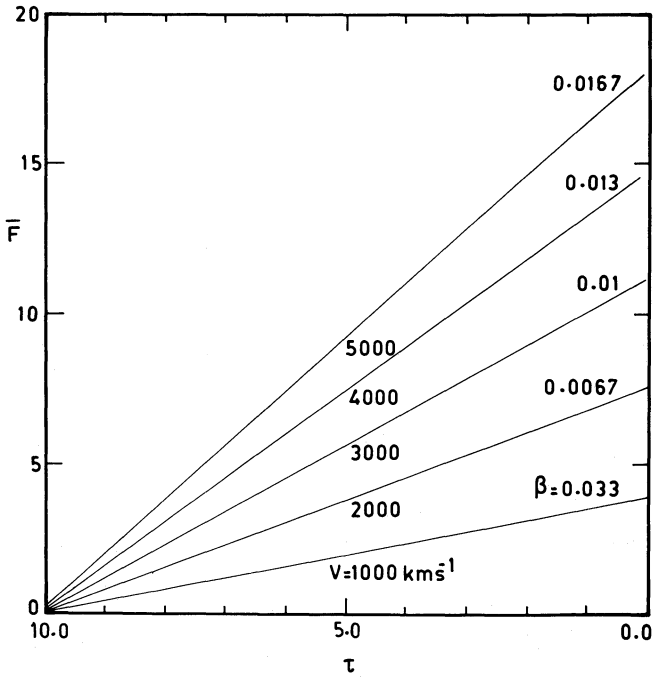

FIG. 10.—$\bar{F}$ plotted for $\tau_{max} = 10$ for positive velocities

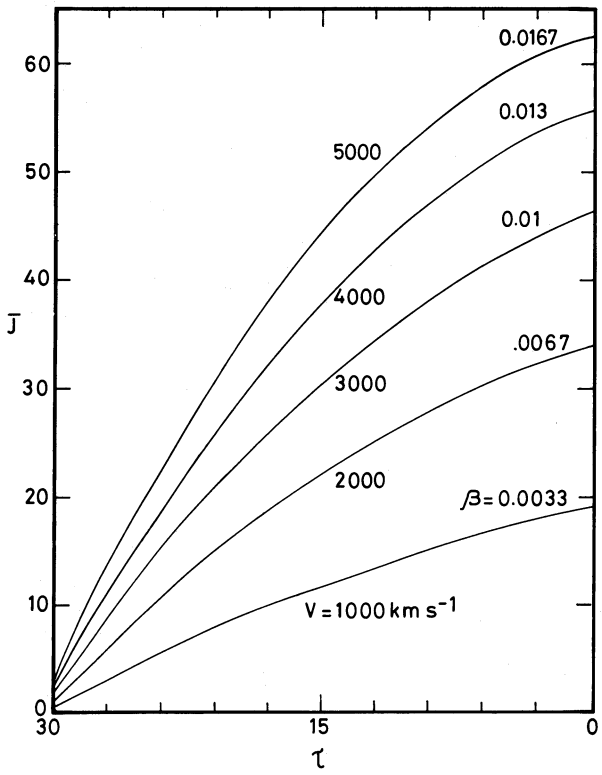

FIG. 11.—$\bar{J}$ plotted for $\tau_{max} = 30$ for positive velocities

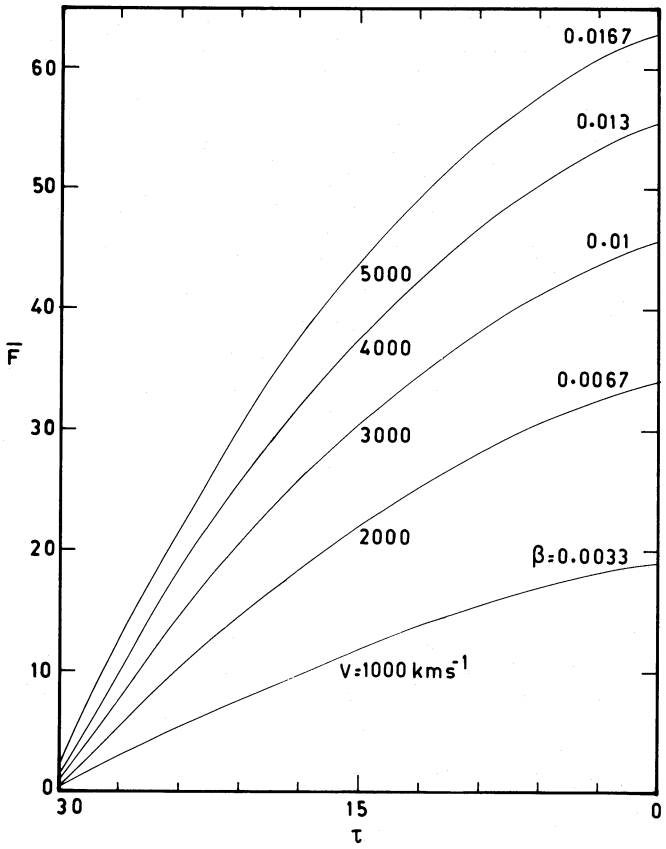

FIG. 12.—$\bar{F}$ plotted for $\tau_{max} = 30$ for positive velocities

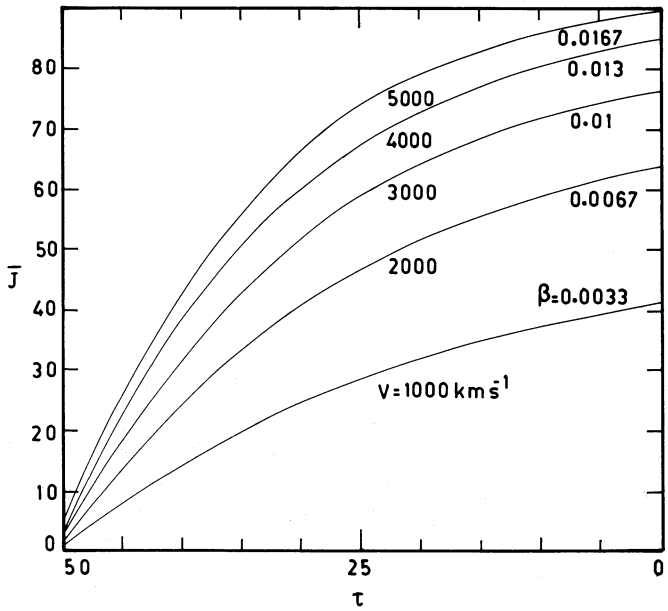

FIG. 13.—$\bar{J}$ plotted for $\tau_{max} = 50$ for positive velocities

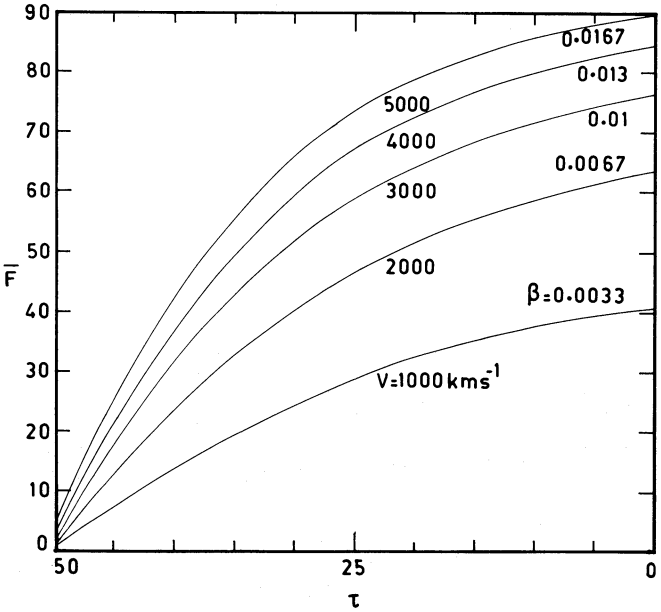

FIG. 14.—$\bar{F}$ plotted for $\tau_{max} = 50$ for positive velocities

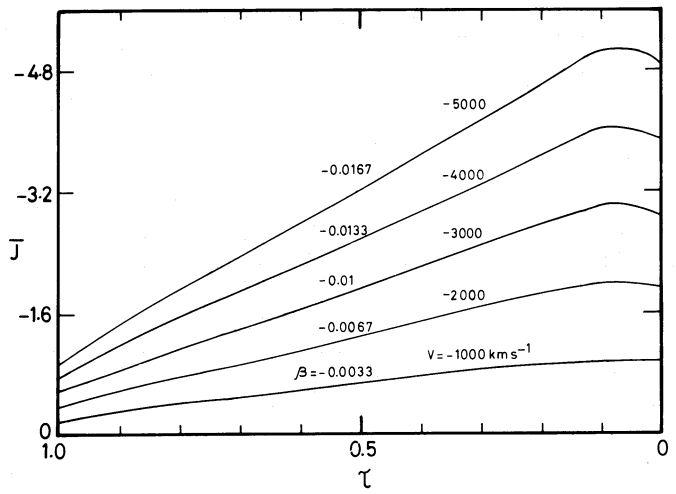

FIG. 15.—$\bar{J}$ plotted for $\tau_{max} = 1$ for negative velocities

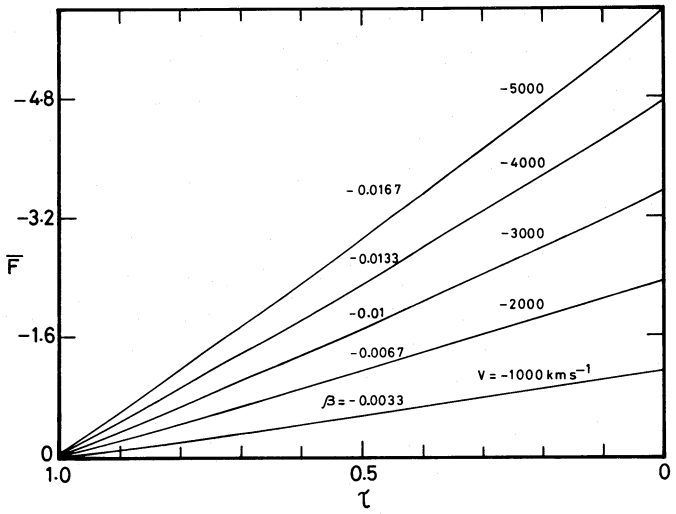

FIG. 16.—$\bar{F}$ plotted for $\tau_{max} = 1$ for negative velocities

So far, positive velocities have been used to calculate the changes in $\bar{J}$ and $\bar{F}$, due to aberration and advection. We shall now find out how negative velocities modify the radiation field. We present the values of $\bar{J}$ and $\bar{F}$ for $V = -1000$ to -5000 km s^{-1} ($\beta \approx -0.0033$) to -0.0167) in Figures 15 and 16. These results are similar to those given in Figures 5 and 6 except that $\bar{J}$ and $\bar{F}$ are negative. This means that J and F are enhanced in the case of negative velocities, while they are reduced in the case of positive velocities, in comparison with those of the medium at rest. The values of $\bar{J}$ and $\bar{F}$ for $\tau_{max} = 5$ and several values of β are presented in Figures 17 and 18. The changes are in the order of -2% at $V = -1000$ km s^{-1}, while at $V = -5000$ km s^{-1} these changes reach a maximum of -13%. For $\tau_{max} = 10$, the change in $\bar{J}$ and $\bar{F}$ are of order -23% (Figs. 19 and 20). In Figures 21 and 22 we plot $\bar{J}$ and $\bar{F}$, and we see that the changes range from -15% at $V = -1000$ km s^{-1} to 85% at $V = -5000$ km s^{-1}. For $\tau_{max} = 50$, $\bar{J}$ and $\bar{F}$ change from -25% to -170% for $V = -1000$ to -5000 km s^{-1} (see Figs. 23 and 24). We see that, as the velocities are increased, the changes introduced in the radiation field are substantial.

We plot the amplification factors $J_{max}/100\beta$ and $F_{max}/100\beta$ versus total thickness of the slab τ for positive velocities in Figures 25 and 26 and for negative velocities in Figures 27 and 28. (This was suggested by the referee.) The amplification factor for positive velocities increases with increasing thickness of the plane-parallel slab. The increase at smaller velocities is higher than that at large velocities. The increase in the amplification factor with the thickness of the slab has already been noticed previously. The higher values for the amplification factor for smaller velocities appears to be nothing but a numerical artifact. In Figures 27 and 28 we plot the amplification factor for negative velocities. The results are similar to those given in Figures 25 and 26.

These results show that in optically thick media, which occur so frequently in nature, even velocities as small as 1000 km s^{-1} change the radiation field considerably. Therefore it is imperative that effects due to aberration and advection be properly considered in evaluating the radiation field.

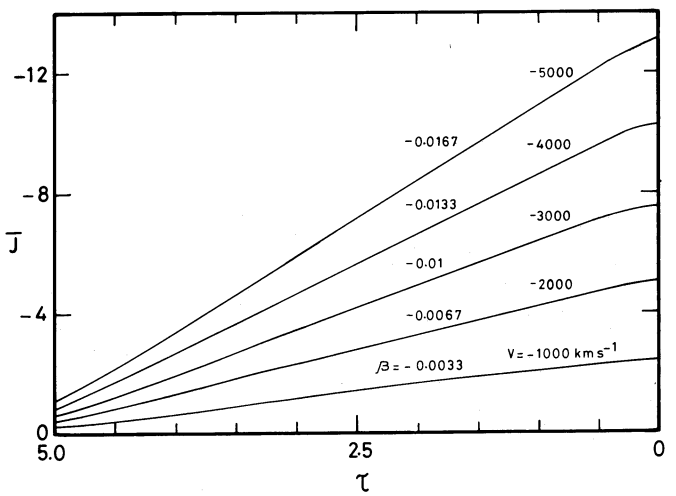

FIG. 17.—$\bar{J}$ plotted for $\tau_{max} = 5$ for negative velocities

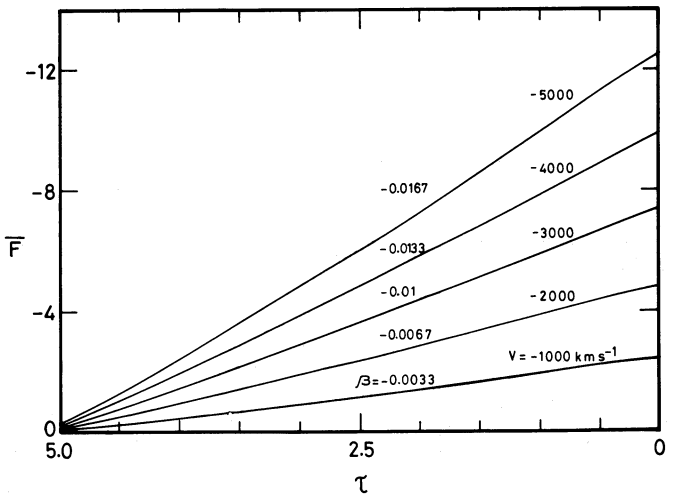

FIG. 18.—$\bar{F}$ plotted for $\tau_{max} = 5$ for negative velocities

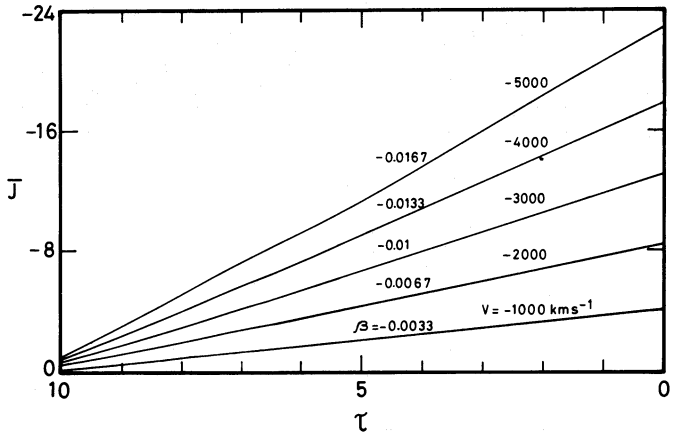

FIG. 19.—$\bar{J}$ plotted for $\tau_{max} = 10$ for negative velocities

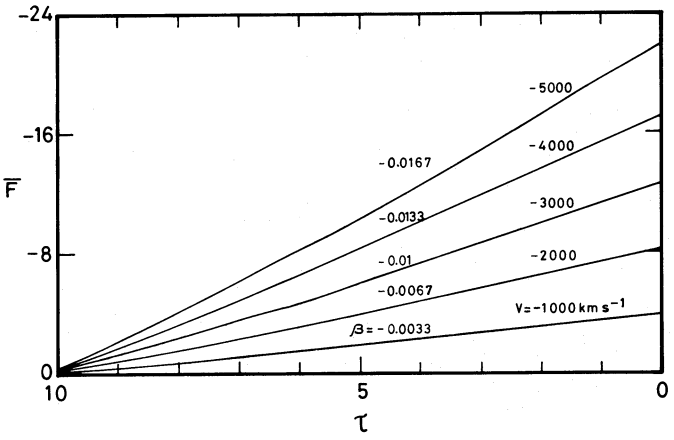

FIG. 20.—$\bar{F}$ plotted for $\tau_{max} = 10$ for negative velocities

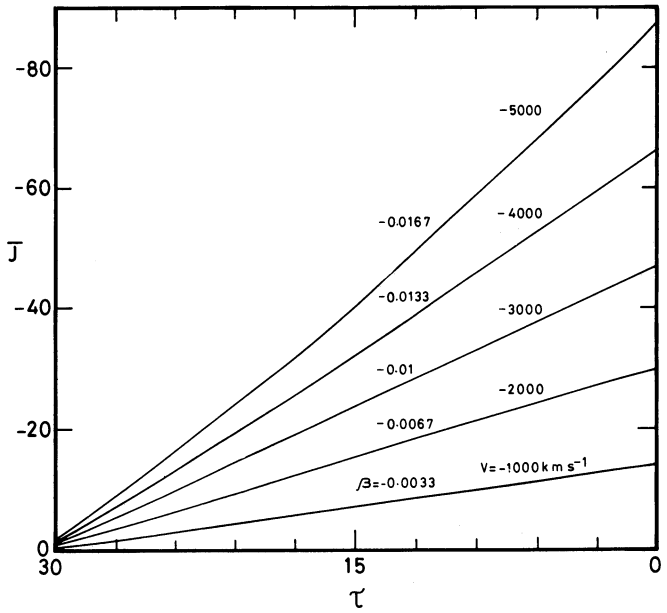

FIG. 21.—$\bar{J}$ plotted for $\tau_{max} = 30$ for negative velocities

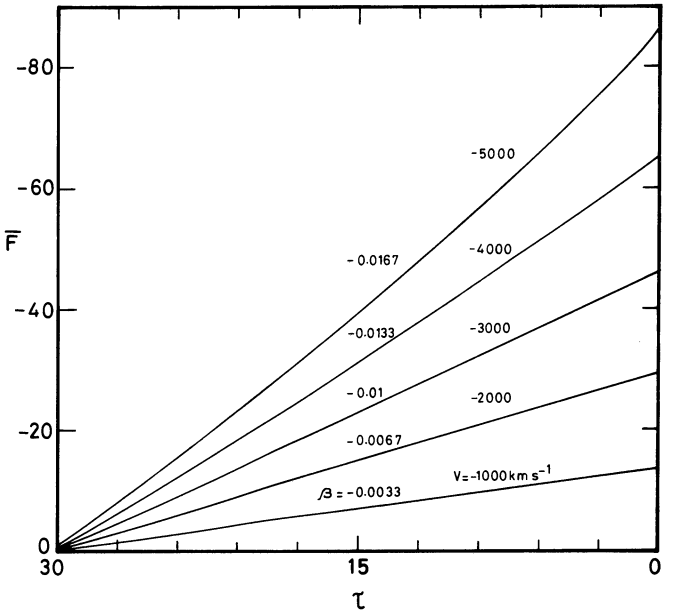

FIG. 22.—$\bar{F}$ plotted for $\tau_{max} = 30$ for negative velocities

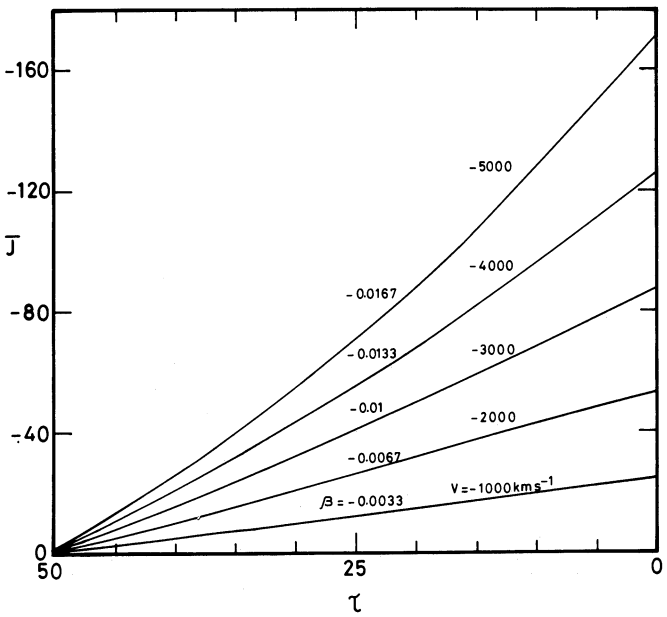

FIG. 23.—$\bar{J}$ plotted for $\tau_{max} = 50$ for negative velocities

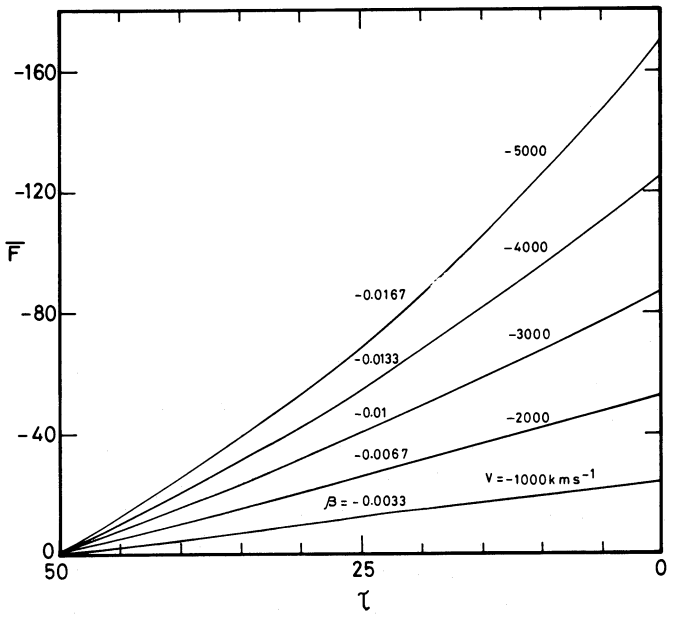

FIG. 24.—$\bar{F}$ plotted for $\tau_{max} = 50$ for negative velocities

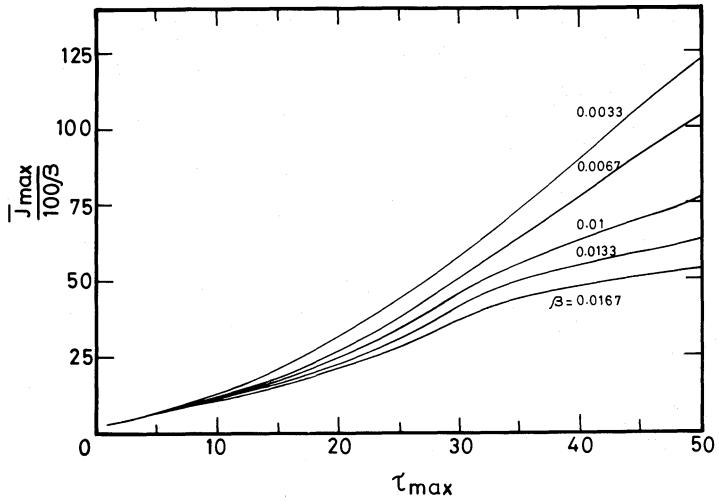

FIG. 25.—Amplification factor $\bar{J}_{max}/100\beta$ vs. τ_{max} for positive velocities

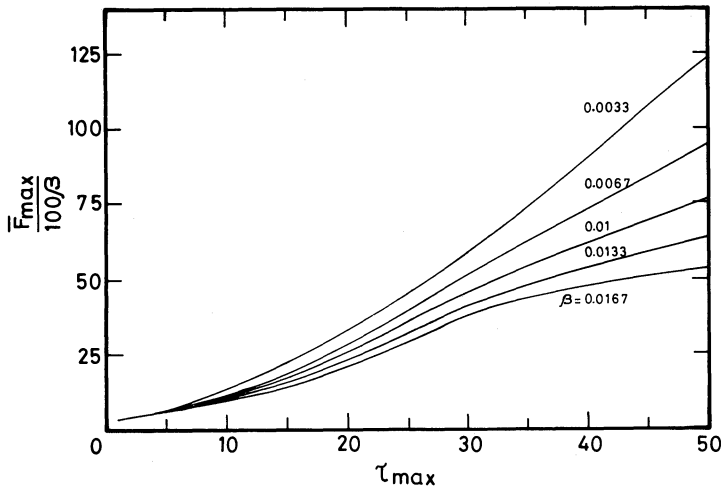

FIG. 26.—Amplification factor $\bar{F}_{max}/100\beta$ vs. τ_{max} for positive velocities

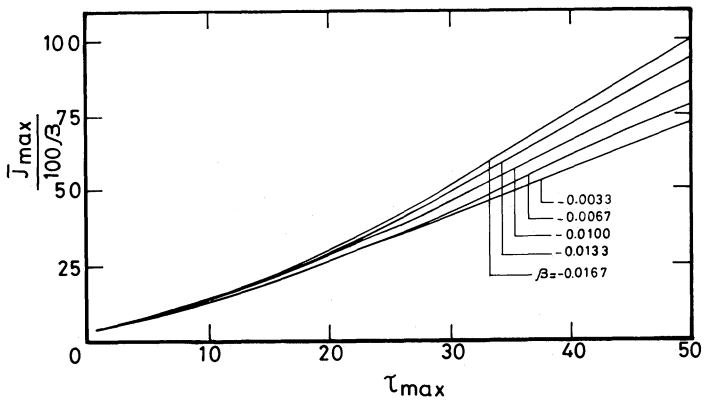

FIG. 27.—Same as Fig. 25, with negative velocities

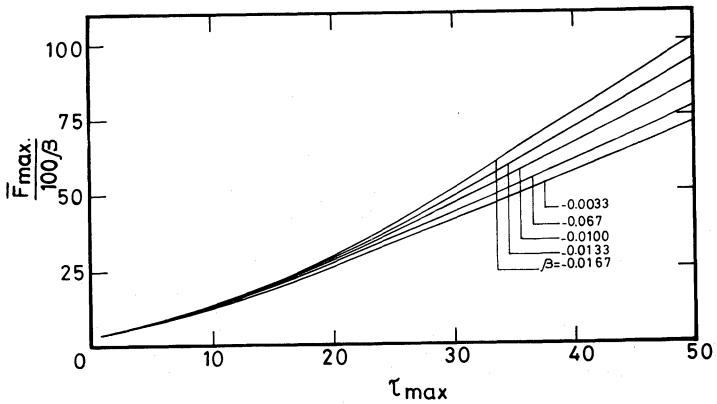

FIG. 28.—Same as Fig. 26, with negative velocities

IV. CONCLUSIONS

We have solved the transfer equation in a moving medium stratified in plane-parallel layers taking into account the aberration and advection terms and assuming coherent and isotropic scattering. We find substantial changes in the mean intensities and outward fluxes due to the above terms.

The author wishes to record his thanks to the referee for comments and criticisms which improved the quality of the paper considerably.

APPENDIX A

NODAL VALUES OF THE ANGLE-RADIUS MESH

The nodal values A_a, A'_a, etc., given in equations (12) and (13) in the text, are given below:

$$A_a = \tau + a_1 + b_1 - c_1 , \qquad A'_a = \tau - a_2 + b_1 - c_2 ,$$
$$A_b = \tau - a_1 + b_2 - c_1 , \qquad A'_b = \tau + a_2 + b_2 - c_2 ,$$
$$A_c = \tau - a_2 + b_1 + c_1 , \qquad A'_c = \tau + a_1 + b_1 + c_2 ,$$
$$A_d = \tau + a_2 + b_2 + c_1 , \qquad A'_d = \tau - a_2 + b_2 + c_2 ,$$

where

$$a_1 = \Delta\mu(\tfrac{1}{3} - \Delta\beta\,\bar{\mu}) , \quad b_1 = \Delta\beta(\overline{3\mu^2} - g) , \quad c_1 = 2(\beta + \bar{\mu}) ,$$
$$a_2 = \Delta\mu(\tfrac{1}{3} + \Delta\beta\,\bar{\mu}) , \quad b_2 = \Delta\beta(\overline{3\mu^2} + g) , \quad c_2 = 2(\beta - \bar{\mu}) ,$$
$$\Delta\beta = (\beta_{n+1} - \beta_n) .$$

APPENDIX B

TRANSMISSION AND REFLECTOR OPERATORS

The two pairs of transmission and reflection operators are given by

$$\boldsymbol{t}(i, i-1) = \boldsymbol{R}^{+-}[\Delta^{+}\boldsymbol{A} + \boldsymbol{r}^{+-}\Delta^{-}\boldsymbol{C}] , \qquad \boldsymbol{t}(i-1, i) = \boldsymbol{R}^{-+}[\Delta^{-}\boldsymbol{D} + \boldsymbol{r}^{-+}\Delta^{+}\boldsymbol{B}] ,$$
$$\boldsymbol{r}(i, i-1) = \boldsymbol{R}^{-+}[\Delta^{-}\boldsymbol{C} + \boldsymbol{r}^{-+}\Delta^{+}\boldsymbol{A}] , \qquad \boldsymbol{r}(i-1, i) = \boldsymbol{R}^{+-}[\Delta^{+}\boldsymbol{B} + \boldsymbol{r}^{+-}\Delta^{-}\boldsymbol{D}] ,$$

where

$$\Delta^{+} = (\bar{\boldsymbol{A}}_{cd} - \tau\boldsymbol{\gamma}^{++})^{-1} , \qquad \Delta^{-} = (\bar{\boldsymbol{A}}_{ab} - \tau\boldsymbol{\gamma}^{--})^{-1} ,$$
$$\bar{\boldsymbol{A}}_{ab} = \boldsymbol{Q}^{-1}\bar{\boldsymbol{A}}^{ab} , \qquad \boldsymbol{A} = \tau\boldsymbol{\gamma}^{++} - \bar{\boldsymbol{A}}_{ab} ,$$
$$\bar{\boldsymbol{A}}'_{ab} = \boldsymbol{Q}^{-1}\bar{\boldsymbol{A}}'_{cd} , \qquad \boldsymbol{B} = \tau\boldsymbol{\gamma}^{+-} ,$$
$$\bar{\boldsymbol{A}}_{cd} = \boldsymbol{Q}^{-1}\bar{\boldsymbol{A}}^{cd} , \qquad \boldsymbol{C} = \tau\boldsymbol{\gamma}^{-+} ,$$
$$\bar{\boldsymbol{A}}'_{ab} = \boldsymbol{Q}^{-1}\bar{\boldsymbol{A}}'_{ab} , \qquad \boldsymbol{D} = \tau\boldsymbol{\gamma}^{++} - \bar{\boldsymbol{A}}'_{cd} ,$$
$$\boldsymbol{r}^{+-} = \tau\Delta^{+}\boldsymbol{\gamma}^{+-} \qquad \boldsymbol{R}^{+-} = [\boldsymbol{I} - \boldsymbol{r}^{+-}\boldsymbol{r}^{-+}]^{-1} .$$

The quantities $\boldsymbol{r}^{-+}$, $\boldsymbol{R}^{-+}$ are obtained by interchanging the signs " + " and " − " in $\boldsymbol{r}^{+-}$ and $\boldsymbol{R}^{+-}$.

REFERENCES

Castor, J. H. 1972, *Ap. J.*, **178**, 779.
Mihalas, D. 1978, *Stellar Atmospheres* (San Francisco: Freeman).
Mihalas, D., and Klein, R. I. 1982, *J. Comput. Phys.*, **46**, 97.
Mihalas, D., Kunasz, P. B., and Hummer, D. G. 1976, *Ap. J.*, **206**, 515.
Munier, A., and Weaver, R. 1986, preprint.
Peraiah, A. 1984, *Methods in Radiative Transfer*, ed. W. Kalkofen (Cambridge: Cambridge University Press), p. 281.
Peraiah, A., and Varghese, B. A. 1985, *Ap. J.*, **290**, 411 (Paper I).

A. PERAIAH: Indian Institute of Astrophysics, Bangalore 560034, India